frontiers | Frontiers in Astronomy and Space Sciences

TYPE Data Report
PUBLISHED 14 May 2024
DOI 10.3389/fspas.2024.1388307

OPEN ACCESS

EDITED BY
Steven Petrinec,
Lockheed Martin Solar and Astrophysics Laboratory (LMSAL), United States

REVIEWED BY
José Juan González-Avilés,
National Autonomous University of Mexico, Mexico
Megha Pandya,
NASA Goddard Space Flight Center, United States

*CORRESPONDENCE
Adrian Pöppelwerth,
a.poeppelwerth@tu-braunschweig.de

RECEIVED 19 February 2024
ACCEPTED 12 April 2024
PUBLISHED 14 May 2024

CITATION
Pöppelwerth A, Koller F, Grimmich N, Constantinescu D, Glebe G, Vörös Z, Temmer M, Simon Wedlund C and Plaschke F (2024), Cluster: List of plasma jets in the subsolar magnetosheath.
Front. Astron. Space Sci. 11:1388307.
doi: 10.3389/fspas.2024.1388307

Cluster: List of plasma jets in the subsolar magnetosheath

Adrian Pöppelwerth[1]*, Florian Koller[2], Niklas Grimmich[1], Dragos Constantinescu[1,3], Georg Glebe[1,4], Zoltán Vörös[5,6], Manuela Temmer[2], Cyril Simon Wedlund[5] and Ferdinand Plaschke[1]

[1]Institute of Geophysics and Extraterrestrial Physics, Technische Universität Braunschweig, Braunschweig, Germany, [2]Institute of Physics, University of Graz, Graz, Austria, [3]Institute of Space Sciences, Magurele, Romania, [4]School of Earth and Atmospheric Sciences, Georgia Institute of Technology, Atlanta, GA, United States, [5]Space Research Institute, Austrian Academy of Sciences, Graz, Austria, [6]Institute of Earth Physics and Space Science, HUN-REN, Sopron, Hungary

KEYWORDS

magnetosheath jets, Cluster, subsolar magnetosheath, dataset, magnetospheric physics

1 Introduction

The Earth's magnetopause, the boundary between the terrestrial and the interplanetary magnetic field (IMF), arises from the interaction of the geomagnetic field with the super-magnetosonic solar wind (on the order of 400–700 km/s; for details, e.g., Hajra, 2023). Upstream, at the bow shock, the solar wind is decelerated to sub-magnetosonic speeds (on the order of 100 km/s; e.g., Soucek and Escoubet, 2012) in order to flow around the magnetopause. The bow shock can be divided into a quasi-parallel ($\theta_{Bn} \lesssim 45°$) and a quasi-perpendicular ($\theta_{Bn} \gtrsim 45°$) shock depending on the angle θ_{Bn} between the shock surface normal and the IMF (Balogh et al., 2005). Solar wind particles can be reflected at the quasi-parallel shock and travel upstream, where they interact with the incoming solar wind. This results in a spatially extended and complex foreshock region that gives birth to instabilities and waves (Eastwood et al., 2005). The three main instabilities driven by the ion/ion beam interaction are called the right- and left-hand resonant and the right-hand non-resonant ion/ion instabilities. At the Earth's foreshock, spacecraft have observed numerous ultralow-frequency waves excited by these instabilities, such as 30-s waves, Alvén/ion cyclotron waves, shocklets, and short large-amplitude magnetic structures (SLAMS) (e.g., Wilson III, 2016). These waves travel back to the shock with the solar wind, causing the quasi-parallel shock to ripple and wave.

In the magnetosheath, which is the region between the bow shock and the magnetopause, we can abundantly and ubiquitously observe dynamic pressure enhancements, which are often referred to as magnetosheath jets (for a comprehensive review, see Plaschke et al., 2018). They occur more often behind the quasi-parallel shock, which corresponds to low IMF cone angles in the subsolar region (e.g., Vuorinen et al., 2019). One of the scenarios to explain the formation of magnetosheath jets is discussed by Hietala et al. (2009, 2012), who pointed out the indentations of the quasi-parallel bow shock. In regions where the local bow shock normal and the solar wind velocity are perpendicular to each other, the plasma is less decelerated and heated while still being compressed. This leads to an increase in dynamic pressure. Other authors have suggested solar wind discontinuities interacting with the shock (Archer et al., 2012), shock reformation (Raptis et al., 2022), hot flow anomalies (HFAs, Savin et al., 2012), or foreshock structures like SLAMS (Karlsson et al., 2018; Suni et al., 2021) as possible mechanisms for the jet formation.

There has been a significant effort in the past 10 years to study jet formation, their occurrence (e.g., LaMoury et al., 2021; Koller et al., 2023), and properties (Raptis et al., 2020). Their scale sizes are in the order of 1 R_E (Gunell et al., 2014; Plaschke et al., 2020), and they have to persist for several minutes to reach the magnetopause. Furthermore, there have been recent studies about waves at jets, e.g., whistler waves due to butterfly pitch angle distributions (Krämer et al., 2023) or lower hybrid waves that may be generated due to density gradients at the edges of jets (Gunell et al., 2014). On the other hand, jet evolution on its way through the magnetosheath is still poorly understood. Plaschke et al. (2017) reported stirring of the ambient plasma and a tendency toward alignment of plasma velocity and magnetic field within jets. Palmroth et al. (2021) conducted multiple global simulation runs to examine their temporal evolution. They observed that jets become more "magnetosheath-like" on their way through the magnetosheath due to decreasing density and velocity and increasing temperature. Although they showed that the properties of the simulated jets are in quantitative agreement with Magnetospheric Multiscale mission (MMS, Burch et al., 2016) observations, there is no observational study showing the temporal evolution of jets.

Although there are multi-spacecraft observations of single-plasma jets (Plaschke and Hietala, 2018), the small inter-spacecraft separations pertaining to individual missions do not allow for an evaluation of the jets' evolution over their lifetime. The inter-spacecraft distances range from a few 100 km to 2 R_E for Time History of Events and Macroscale Interactions during Substorms (THEMIS) (Angelopoulos et al., 2008), 3 km to 10 R_E with an average separation of approximately 1,000 km for Cluster (Escoubet et al., 2001), and 10–400 km for MMS at the beginning of the mission (Burch et al., 2016). Therefore, it is advantageous to use conjunctions of spacecraft from different missions to study jets, as Escoubet et al. (2020) did for a case study with MMS and Cluster. This makes it possible to investigate a jet at different times on its way from the bow shock to the magnetopause. To facilitate these kinds of studies, it is useful to have lists of jet observations from different space missions. As these jet lists already exist for MMS (Raptis et al., 2020) and THEMIS (Plaschke et al., 2013; LaMoury et al., 2021; Koller et al., 2022), we saw the need to create a list for the Cluster mission. The additional list also has the advantage of providing more opportunities to study jets; this is important as we still do not know how significant their impact on the magnetosphere is.

The Cluster mission, consisting of four spacecraft, was launched in 2000 and is designed to investigate small-scale structures and macroscopic turbulence in three dimensions that occur in many places of the magnetosphere. The spacecraft are on highly elliptical and polar orbits of 4×19.6 R_E and are equipped with 11 instruments to investigate particles and fields (Escoubet et al., 2001).

Echim et al. (2023) already investigated a dataset of 960 jets detected by Cluster using an adapted method following Archer and Horbury (2013). They reported a dawn–dusk asymmetry in the temperature and density of magnetosheath jets. However, the authors examined Cluster measurements from 2007 to 2008; we provide a list of subsolar dayside jet detections for the entire mission duration from 2000 to 2023. In addition, we provide lists for multiple detection criteria.

2 Methods

To infer the upstream solar wind parameters, we made use of the high-resolution (1 min) OMNI database (King and Papitashvili, 2005) and obtained solar wind speed, density, and IMF values propagated to the bow shock nose. On board Cluster, we used ion measurements from the Hot Ion Analyzer of the Cluster Ion Spectrometry experiment (CIS-HIA, Rème et al., 2001) with a time resolution of 4s to obtain ion velocity, ion density, and the ion omnidirectional energy flux density. As CIS-HIA was only operational on spacecraft C1 and C3, we were not able to detect jets with C2 and C4 (Dandouras et al., 2010).

To detect jets at the dayside subsolar magnetosheath, we had to identify the corresponding magnetosheath intervals in the spacecraft data. In order to do this, we investigated Cluster data sampled between 7 and 18 R_E from Earth's center in a 30°-wide cone oriented to the Sun with the tip at Earth's center. In this region, the ion density must surpass twice the value measured in the solar wind. In addition, the ion omnidirectional energy flux density of the 1 keV ions must be higher than that of the 10 keV ions in order to exclude measurements in the magnetosphere (Plaschke et al., 2013).

As we aimed to compare our results with previous works, we used the same jet detection criteria in those works. There are mainly three different detection methods: those of Archer and Horbury (2013) (i), Koller et al. (2022) (ii), and Plaschke et al. (2013) (iii). We briefly recap the criteria used to detect jets in our magnetosheath intervals but refer to the above studies for a detailed description. We denoted the start and end times of the jet as t_{start} and t_{end}, respectively, and the time of the maximum dynamic pressure P_{dyn} as t_0. The time intervals 1 minute before and after the jet interval are called "pre"- and "post-jet" intervals, respectively, and must also lie in the magnetosheath interval for all three criteria (i–iii).

(i) For the detection after Archer and Horbury (2013), we compared the dynamic pressure in the magnetosheath P_{dyn} with the 20-min average of the magnetosheath dynamic pressure $\langle P_{dyn} \rangle_{20min}$. Jet intervals were identified, where P_{dyn} increased above $2 \cdot \langle P_{dyn} \rangle_{20min}$.

(ii) Following the detection method in Koller et al. (2022), we searched for times when the dynamic pressure in the magnetosheath in the GSE-X direction $P_{dyn,x}$ exceeded three times the 20-min average of the dynamic pressure in the GSE-X direction $\langle P_{dyn,x} \rangle_{20min}$. t_{start} and t_{end} of the jet intervals were defined, where $P_{dyn,x}$ increased above twice $\langle P_{dyn,x} \rangle_{20min}$. In addition, the detection methods (ii) and (iii) require that the GSE-X component of the ion velocity V_x must remain negative during the entire jet interval, and V_x has to be greater than $V_x(t_0)/2$ at least once within the pre-and post-jet intervals.

(iii) Finally, we followed Plaschke et al. (2013) and searched in our subsolar magnetosheath intervals for times when $P_{dyn,x}$ was surpassing half the solar wind dynamic pressure $P_{dyn,sw}$. t_{start} and t_{end} of the corresponding jet interval were determined, where $P_{dyn,x}$ equaled one quarter of $P_{dyn,sw}$.

Furthermore, the jet intervals for (i)–(iii) were required to last longer than the mean proton cyclotron period in the corresponding magnetosheath interval, as very short jets could be just fluctuations due to the normal magnetosheath turbulence.

We applied the abovementioned criteria to identify magnetosheath jets from the beginning of the Cluster mission through the end of 2023. This corresponds to the period from 01 January 2000 to 31 December 2023. In a preliminary investigation, we looked at the spatial distribution of the spacecraft that detect the jets. To compare the positions for different solar wind conditions, we used statistical model boundaries for magnetopause and bow shock to calculate the relative position r_{rel} within the magnetosheath (cf. Archer and Horbury, 2013):

$$r_{rel} = \frac{r - r_{MP}}{r_{BS} - r_{MP}}. \quad (1)$$

Here, r_{BS} and r_{MP} denote the radial distances of the bow shock and magnetopause along the Earth–spacecraft line, respectively, whereas r is the radial distance of the observing spacecraft. $r_{rel} = 0$ and $r_{rel} = 1$ correspond to a spacecraft at the magnetopause and the bow shock, respectively. We used the symmetric magnetopause model by Shue et al. (1998):

$$r_{MP} = r_{0,MP}\left(\frac{2}{1+\cos\theta}\right)^{\alpha}, \quad (2)$$

where $r_{0,MP}$ and α are the standoff distance and the level of tail flaring, respectively; and θ is the cone angle from the GSE-X-axis. For the bow shock, we used the model by Chao et al. (2002):

$$r_{BS} = r_{0,BS}\left(\frac{1+\epsilon}{1+\epsilon\cos\theta}\right)^{\alpha}, \quad (3)$$

where $r_{0,BS}$ is the standoff distance of the bow shock, ϵ is a parameter similar to the eccentricity and describes the curvature of the model bow shock, θ is the cone angle from the aberrated GSE-X-axis, and α is the same as in the magnetopause model.

3 Data

We found 2,233 measurement intervals in the subsolar magnetosheath, containing 780 h of data in total. Applying the different detection criteria led to 2,771 jets for the method by (i), 864 jets by (ii), and 1,408 jets by (iii). We provide detailed information about the number of jets and the observation time in the magnetosheath for different years in Figure 1. Figure 1A shows the number of detected jets per year for the criteria of (i), (ii), and (iii) in orange, red, and blue, respectively. Figure 1B shows the yearly observation time of jets normalized by the observation time in the magnetosheath with the same colors for the three criteria. Figure 1C shows the magnetosheath observation time per year in black.

Lists containing interval times for observing spacecraft and the magnetosheath interval times are available at https://osf.io/xvdy6 (Pöppelwerth et al., 2024). In addition, we made use of the provided ancillary data on the CIS-HIA instrument; for each magnetosheath and jet interval, we provided the minimum value of the quality flag value, which indicated potential problems that could affect the detailed analysis of the data (for more information on quality flags and caveats, see Dandouras et al., 2010). Since the beginning of 2015, the quality flag is no longer available and requires the user to be careful with the use of the data for a detailed analysis. Since we only observed 21 jets afterward, this issue did not have a major impact.

Figure 1 shows that the number of jets decreased rapidly after 2010. The reasons for the lower number of jet detections are the aging effects of the Cluster spacecraft instruments. The CIS-HIA onboard C3 has not been operational since 11 November 2009. The operational time onboard C1 was limited to 1 hour per orbit from November 2012 to December 2016, when more frequent operations were adopted for CIS-HIA on C1 up to 2×1 h per orbit (Dandouras and Barthe, 2024). We also noted that there are no subsolar magnetosheath intervals after March 2017, when all data products were available. Therefore, we did not observe any jets after 2017. The absence of subsolar magnetosheath intervals can be explained by the fact that these short operating time intervals lie near the magnetopause and often within the magnetosphere.

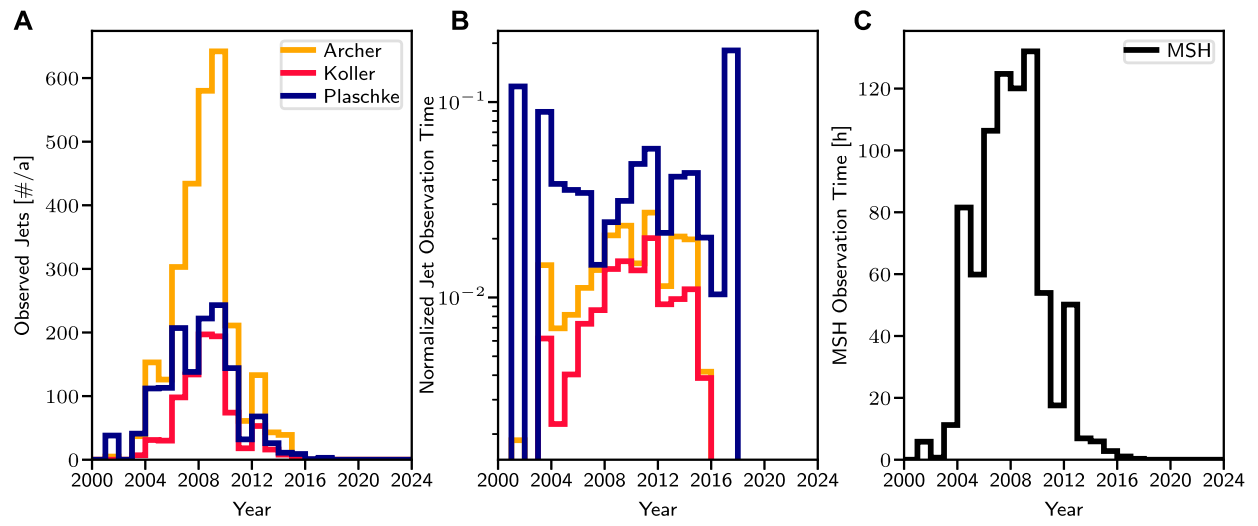

FIGURE 1
In panels **(A,B)**, the data for Archer and Horbury (2013), Koller et al. (2022), and Plaschke et al. (2013) criteria are shown in orange, red, and blue, respectively. **(A)** Number of detected jets per year in the subsolar magnetosheath for all three detection criteria. **(B)** Time of jet observation per year normalized by the time of magnetosheath observation. **(C)** Observation time in the magnetosheath per year.

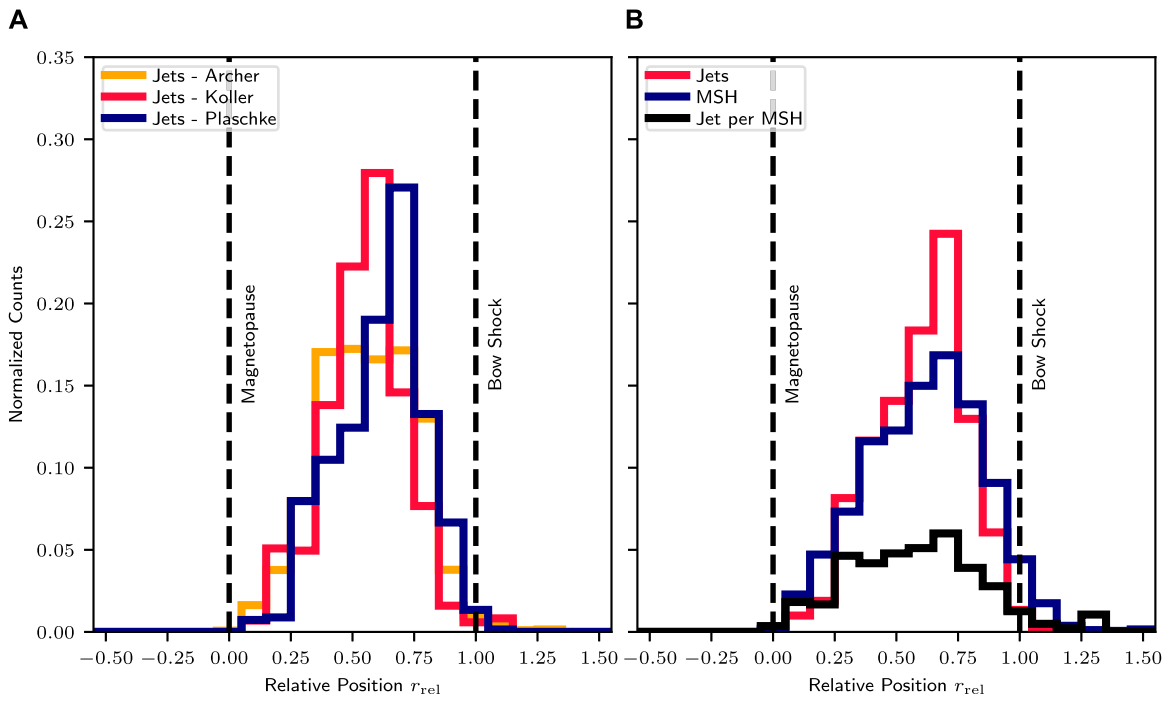

FIGURE 2
(A) Relative positions r_{rel} of detected jets in the magnetosheath for all three detection criteria. The distributions for Archer and Horbury (2013), Koller et al. (2022), and Plaschke et al. (2013) are shown in orange, red, and blue, respectively. **(B)**: Relative positions r_{rel} of all magnetosheath and all jet observations in red and blue, respectively. Also shown is the distribution of jet observations normalized to the magnetosheath distribution in black.

In addition, as per Figure 1A (orange), more jets were detected with the criteria by Archer and Horbury (2013), since the authors also considered purely density-driven jets, and did not apply a threshold to the velocity. Their criterion is, therefore, not as strict as those of Koller et al. (2022) or Plaschke et al. (2013). Furthermore, the jets detected with criterion (i) with a mean duration of 14 s were on average shorter than those detected with criteria (ii) and (iii) with mean durations of 31 s and 62 s, respectively.

The spatial distributions of spacecraft detecting jets with the three different detection criteria from Archer and Horbury (2013), Koller et al. (2022), and Plaschke et al. (2013) are shown in Figure 2A in orange, red, and blue, respectively. In addition, we show the spatial distribution of all detected jets (Archer + Koller + Plaschke) and magnetosheath observations together with the distribution of jet observations normalized to the magnetosheath distribution in Figure 2B. Here, we have filtered out multiple counts of the same jets if they were detected by multiple criteria.

Evidently, the majority of jets are found in the middle of the magnetosheath and near and, apparently, even upstream of the bow shock (Figure 2A and red histogram in Figure 2B). The median values of the relative position r_{rel} (Eq. 1) for jets detected by Archer and Horbury (2013), Koller et al. (2022), and Plaschke et al. (2013) criteria are 0.58, 0.56, and 0.65, respectively. Jet detections and magnetosheath intervals within the magnetosphere or the solar wind are due to the statistical nature of our model boundaries (Eqs 2, 3) which do not represent all cases perfectly. The majority of magnetosheath observations were also taken in the middle of the magnetosheath and closer to the bow shock (blue histogram in Figure 2B). To remove the orbital bias, we divided the jet observations by the magnetosheath observations (black histogram in Figure 2B). The median values of the relative position r_{rel} for all jet and magnetosheath observations were 0.62 and 0.63, respectively.

The biased distributions of the absolute values of jet detections (Figure 2A and red histogram in Figure 2B) differ from the spatial distribution of jets detected by THEMIS (e.g., Fig. 3 in Plaschke et al., 2013) and MMS (e.g., Fig. 3 in Raptis et al., 2020), as these authors observed jets more often located near the magnetopause. This follows reasonably from the given orbits of the various missions. Cluster has a highly elliptical orbit with the apogees on the dayside located farther away from Earth than the inner THEMIS probes (THA, THD, and THE) or MMS in phase 1 (Angelopoulos, 2008; Fuselier et al., 2016; Escoubet et al., 2021). These complementary observations can, therefore, pave the way to understand the evolution of jets traveling through the magnetosheath.

4 Conclusions

In this paper, we present lists of magnetosheath jet observations in the Earth's dayside subsolar magnetosheath for the Cluster mission using three different selection criteria. In total, there are 2,771 jets for the Archer and Horbury (2013) method, 864 jets for the Koller et al. (2022) method and 1,408 jets for the Plaschke et al. (2013) method.

The spatial distribution of the detected jets deviates from other missions like THEMIS and MMS, thus allowing future studies of jet evolution with spacecraft conjunctions from different missions. Potential future work involves identifying cases for conjunctions, although this will require a significant amount of additional effort. One has to consider the times, spacecraft positions, and the propagation directions of the jets. Furthermore, we need to take into account possible time delays as the jets move through the magnetosheath. As Cluster was launched 7 years before THEMIS, it is also possible to further investigate the dependence of the solar cycle on jet occurrence, following the pioneering work of Vuorinen et al. (2023).

It should be noted, however, that care has to be taken when comparing jets detected by different spacecraft missions. The instrumentation on board the various spacecraft may be different in terms of resolution, calibration, and age. Therefore, a direct comparison of quantities is only possible to a certain degree and requires special attention.

Data availability statement

The original contributions presented in the study are publicly available. This data can be found here: osf.io/xvdy6, Database: Cluster - subsolar magnetosheath jet data 2000-2023 (Pöppelwerth et al. (2024)).

Author contributions

AP: conceptualization, data curation, formal analysis, investigation, software, validation, visualization, writing–original draft, and writing–review and editing. FK: conceptualization, methodology, software, validation, and writing–review and editing. NG: software and writing–review and editing. DC: software and writing–review and editing. GG: writing–review and editing. ZV: writing–review and editing. MT: writing–review and editing. CS: writing–review and editing. FP: methodology, software, supervision, and writing–review and editing.

Funding

The author(s) declare that financial support was received for the research, authorship, and/or publication of this article. FK and ZV acknowledge the support of the Austrian Science Fund (FWF), P 33285-N. NG and FP acknowledge the support of the German Center for Aviation and Space (DLR) under contract 50 OC 2401. CS acknowledges the support of the Austrian Science Fund (FWF), FWF project P35954-N.

Acknowledgments

The data from the Cluster mission are publicly available and can be obtained from https://spdf.gsfc.nasa.gov/pub/data/cluster/ (Cluster, 2024). The authors thank Laakso et al. (2010) for their effort to provide the data and user guides. The solar wind data from NASA's OMNI high-resolution dataset (1 min cadence) are also publicly available and can be obtained from https://spdf.gsfc.nasa.gov/pub/data/omni/omni_cdaweb (OMNI, 2024).

Conflict of interest

The authors declare that the research was conducted in the absence of any commercial or financial relationships that could be construed as a potential conflict of interest.

Publisher's note

References

Angelopoulos, V. (2008). The themis mission. *Space Sci. Rev.* 141, 5–34. doi:10.1007/s11214-008-9336-1

Angelopoulos, V., Sibeck, D., Carlson, C. W., McFadden, J. P., Larson, D., Lin, R. P., et al. (2008). First results from the themis mission. *Space Sci. Rev.* 141, 453–476. doi:10.1007/s11214-008-9378-4

Archer, M. O., and Horbury, T. S. (2013). Magnetosheath dynamic pressure enhancements: occurrence and typical properties. *Ann. Geophys.* 31, 319–331. doi:10.5194/angeo-31-319-2013

Archer, M. O., Horbury, T. S., and Eastwood, J. P. (2012). Magnetosheath pressure pulses: generation downstream of the bow shock from solar wind discontinuities. *J. Geophys. Res. Space Phys.* 117. doi:10.1029/2011JA017468

Balogh, A., Schwartz, S. J., Bale, S. D., Balikhin, M. A., Burgess, D., Horbury, T. S., et al. (2005). Cluster at the bow shock: introduction. *Space Sci. Rev.* 118, 155–160. doi:10.1007/s11214-005-3826-1

Burch, J. L., Moore, T. E., Torbert, R. B., and Giles, B. L. (2016). Magnetospheric multiscale overview and science objectives. *Space Sci. Rev.* 199, 5–21. doi:10.1007/s11214-015-0164-9

Chao, J., Wu, D., Lin, C.-H., Yang, Y.-H., Wang, X., Kessel, M., et al. (2002). "Models for the size and shape of the earth's magnetopause and bow shock," in *Space weather study using multipoint techniques*. Editor L.-H. Lyu (Pergamon), 127–135. 12 of COSPAR Colloquia Series. doi:10.1016/S0964-2749(02)80212-8

Cluster (2024). Cluster mission including cis and fgm data. Available at: https://spdf.gsfc.nasa.gov/pub/data/cluster/(last access January 26, 2024).

Dandouras, I., and Barthe, A. (2024). User guide to the cis measurements in the cluster active archive (caa). Available at: https://caa.esac.esa.int/documents/UG/CAA_EST_UG_CIS_v38.pdf (last access January 31, 2024).

Dandouras, I., Barthe, A., Penou, E., Brunato, S., Rème, H., Kistler, L. M., et al. (2010). "Cluster ion spectrometry (CIS) data in the cluster active archive (CAA)," in *The cluster active archive: studying the Earth's space plasma environment* (Springer), 51–72.

Eastwood, J. P., Lucek, E. A., Mazelle, C., Meziane, K., Narita, Y., Pickett, J., et al. (2005). The foreshock. *Space Sci. Rev.* 118, 41–94. doi:10.1007/s11214-005-3824-3

Echim, M., Voiculescu, M., Munteanu, C., Teodorescu, E., Voitcu, G., Negrea, C., et al. (2023). On the phenomenology of magnetosheath jets with insight from theory, modelling, numerical simulations and observations by cluster spacecraft. *Front. Astronomy Space Sci.* 10. doi:10.3389/fspas.2023.1094282

Escoubet, C., Fehringer, M., and Goldstein, M. (2001). The Cluster mission. *Ann. Geophys.* 19, 1197–1200. doi:10.5194/angeo-19-1197-2001

Escoubet, C. P., Hwang, K.-J., Toledo-Redondo, S., Turc, L., Haaland, S. E., Aunai, N., et al. (2020). Cluster and mms simultaneous observations of magnetosheath high speed jets and their impact on the magnetopause. *Front. Astronomy Space Sci.* 6. doi:10.3389/fspas.2019.00078

Escoubet, C. P., Masson, A., Laakso, H., Goldstein, M. L., Dimbylow, T., Bogdanova, Y. V., et al. (2021). Cluster after 20 years of operations: science highlights and technical challenges. *J. Geophys. Res. Space Phys.* 126, e2021JA029474. doi:10.1029/2021JA029474

Fuselier, S. A., Lewis, W. S., Schiff, C., Ergun, R., Burch, J. L., Petrinec, S. M., et al. (2016). Magnetospheric multiscale science mission profile and operations. *Space Sci. Rev.* 199, 77–103. doi:10.1007/s11214-014-0087-x

Gunell, H., Stenberg Wieser, G., Mella, M., Maggiolo, R., Nilsson, H., Darrouzet, F., et al. (2014). Waves in high-speed plasmoids in the magnetosheath and at the magnetopause. *Ann. Geophys.* 32, 991–1009. doi:10.5194/angeo-32-991-2014

Hajra, R. (2023). Near-earth high-speed and slow solar winds: a statistical study on their characteristics and geomagnetic impacts. *Sol. Phys.* 298, 53. doi:10.1007/s11207-023-02141-6

Hietala, H., Laitinen, T. V., Andréeová, K., Vainio, R., Vaivads, A., Palmroth, M., et al. (2009). Supermagnetosonic jets behind a collisionless quasiparallel shock. *Phys. Rev. Lett.* 103, 245001. doi:10.1103/PhysRevLett.103.245001

Hietala, H., Partamies, N., Laitinen, T. V., Clausen, L. B. N., Facskó, G., Vaivads, A., et al. (2012). Supermagnetosonic subsolar magnetosheath jets and their effects: from the solar wind to the ionospheric convection. *Ann. Geophys.* 30, 33–48. doi:10.5194/angeo-30-33-2012

Karlsson, T., Plaschke, F., Hietala, H., Archer, M., Blanco-Cano, X., Kajdič, P., et al. (2018). Investigating the anatomy of magnetosheath jets – mms observations. *Ann. Geophys.* 36, 655–677. doi:10.5194/angeo-36-655-2018

King, J. H., and Papitashvili, N. E. (2005). Solar wind spatial scales in and comparisons of hourly wind and ace plasma and magnetic field data. *J. Geophys. Res. Space Phys.* 110. doi:10.1029/2004JA010649

Koller, F., Plaschke, F., Temmer, M., Preisser, L., Roberts, O. W., and Vörös, Z. (2023). Magnetosheath jet formation influenced by parameters in solar wind structures. *J. Geophys. Res. Space Phys.* 128, e2023JA031339. doi:10.1029/2023JA031339

Koller, F., Temmer, M., Preisser, L., Plaschke, F., Geyer, P., Jian, L. K., et al. (2022). Magnetosheath jet occurrence rate in relation to cmes and sirs. *J. Geophys. Res. Space Phys.* 127, e2021JA030124. doi:10.1029/2021JA030124

Krämer, E., Hamrin, M., Gunell, H., Karlsson, T., Steinvall, K., Goncharov, O., et al. (2023). Waves in magnetosheath jets—classification and the search for generation mechanisms using mms burst mode data. *J. Geophys. Res. Space Phys.* 128, e2023JA031621. doi:10.1029/2023JA031621

Laakso, H., Perry, C., McCaffrey, S., Herment, D., Allen, A. J., Harvey, C. C., et al. (2010). "Cluster active archive: overview," in *The cluster active archive*. Editors H. Laakso, M. Taylor, and C. P. Escoubet (Dordrecht: Springer Netherlands), 3–37.

LaMoury, A. T., Hietala, H., Plaschke, F., Vuorinen, L., and Eastwood, J. P. (2021). Solar wind control of magnetosheath jet formation and propagation to the magnetopause. *J. Geophys. Res. Space Phys.* 126, e2021JA029592. doi:10.1029/2021ja029592

OMNI (2024). Solar wind data from nasa's omni high resolution data set. Available at: https://omniweb.gsfc.nasa.gov/ow_min.html (last access January 26, 2024).

Palmroth, M., Raptis, S., Suni, J., Karlsson, T., Turc, L., Johlander, A., et al. (2021). Magnetosheath jet evolution as a function of lifetime: global hybrid-vlasov simulations compared to mms observations. *Ann. Geophys.* 39, 289–308. doi:10.5194/angeo-39-289-2021

Plaschke, F., and Hietala, H. (2018). Plasma flow patterns in and around magnetosheath jets. *Ann. Geophys.* 36, 695–703. doi:10.5194/angeo-36-695-2018

Plaschke, F., Hietala, H., and Angelopoulos, V. (2013). Anti-sunward high-speed jets in the subsolar magnetosheath. *Ann. Geophys.* 31, 1877–1889. doi:10.5194/angeo-31-1877-2013

Plaschke, F., Hietala, H., Archer, M. O., Blanco-Cano, X., Kajdič, P., Karlsson, T., et al. (2018). Jets downstream of collisionless shocks. *Space Sci. Rev.* 214, 81. doi:10.1007/s11214-018-0516-3

Plaschke, F., Hietala, H., and Vörös, Z. (2020). Scale sizes of magnetosheath jets. *J. Geophys. Res.-Space* 125, e2020JA027962. doi:10.1029/2020JA027962

Plaschke, F., Karlsson, T., Hietala, H., Archer, M., Vörös, Z., Nakamura, R., et al. (2017). Magnetosheath high-speed jets: internal structure and interaction with ambient plasma. *J. Geophys. Res. Space Phys.* 122 (10), 157–175. doi:10.1002/2017JA024471

Pöppelwerth, A., Koller, F., Plaschke, F., Grimmich, N., Constantinescu, D., Glebe, G., et al. (2024). Database: cluster - subsolar magnetosheath jet data 2000-2023. Available at: https://osf.io/xvdy6. doi:10.17605/OSF.IO/XVDY6

Raptis, S., Karlsson, T., Plaschke, F., Kullen, A., and Lindqvist, P.-A. (2020). Classifying magnetosheath jets using mms: statistical properties. *J. Geophys. Res. Space Phys.* 125, e2019JA027754. doi:10.1029/2019JA027754

Raptis, S., Karlsson, T., Vaivads, A., Pollock, C., Plaschke, F., Johlander, A., et al. (2022). Downstream high-speed plasma jet generation as a direct consequence of shock reformation. *Nat. Commun.* 13, 598. doi:10.1038/s41467-022-28110-4

Rème, H., Aoustin, C., Bosqued, J. M., Dandouras, I., Lavraud, B., Sauvaud, J. A., et al. (2001). First multispacecraft ion measurements in and near the earth's magnetosphere with the identical cluster ion spectrometry (cis) experiment. *Ann. Geophys.* 19, 1303–1354. doi:10.5194/angeo-19-1303-2001

Savin, S., Amata, E., Zelenyi, L., Lutsenko, V., Safrankova, J., Nemecek, Z., et al. (2012). Super fast plasma streams as drivers of transient and anomalous magnetospheric dynamics. *Ann. Geophys.* 30, 1–7. doi:10.5194/angeo-30-1-2012

Shue, J.-H., Song, P., Russell, C. T., Steinberg, J. T., Chao, J. K., Zastenker, G., et al. (1998). Magnetopause location under extreme solar wind conditions. *J. Geophys. Res. Space Phys.* 103, 17691–17700. doi:10.1029/98JA01103

Soucek, J., and Escoubet, C. P. (2012). Predictive model of magnetosheath plasma flow and its validation against cluster and themis data. *Ann. Geophys.* 30, 973–982. doi:10.5194/angeo-30-973-2012

Suni, J., Palmroth, M., Turc, L., Battarbee, M., Johlander, A., Tarvus, V., et al. (2021). Connection between foreshock structures and the generation of magnetosheath jets: vlasiator results. *Geophys. Res. Lett.* 48, e2021GL095655. doi:10.1029/2021GL095655

Vuorinen, L., Hietala, H., and Plaschke, F. (2019). Jets in the magnetosheath: imf control of where they occur. *Ann. Geophys.* 37, 689–697. doi:10.5194/angeo-37-689-2019

Vuorinen, L., LaMoury, A. T., Hietala, H., and Koller, F. (2023). Magnetosheath jets over solar cycle 24: an empirical model. *J. Geophys. Res. Space Phys.* 128, e2023JA031493. doi:10.1029/2023JA031493

Wilson III, L. B. (2016). *Low frequency waves at and upstream of collisionless shocks*. American Geophysical Union (AGU, 269–291. chap. 16. doi:10.1002/9781119055006.ch16